



ELSEVIER

<http://dx.doi.org/10.1016/j.ultrasmedbio.2012.08.015>

● *Original Contribution*

## APPLICATIONS OF EXOGENOUS MESENCHYMAL STEM CELLS AND LOW INTENSITY PULSED ULTRASOUND ENHANCE FRACTURE HEALING IN RAT MODEL

WING-HOI CHEUNG,<sup>\*†</sup> WAI-CHING CHIN,<sup>\*</sup> FANG-YUAN WEI,<sup>\*</sup> GANG LI,<sup>\*</sup> and KWOK-SUI LEUNG<sup>\*†</sup>

<sup>\*</sup>Department of Orthopaedics and Traumatology, The Chinese University of Hong Kong, Shatin, New Territories, Hong Kong SAR, China; and <sup>†</sup>Translational Medicine Research and Development Center, Institute of Biomedical and Health Engineering, Shenzhen Institutes of Advanced Technology, Chinese Academy of Sciences, Shenzhen, China

(Received 25 May 2012; revised 10 August 2012; in final form 21 August 2012)

**Abstract**—The present study aimed to investigate the effects of combined treatment of exogenous mesenchymal stem cells (MSCs) and low intensity pulsed ultrasound (LIPUS) on fracture healing by comparing LIPUS-MSC, MSC and control (CTL) groups. Radiography and quantitative callus width/area demonstrated that the MSC-LIPUS group had the best healing, MSC group the second and CTL group the poorest with significant differences among each at different time points. Micro-CT data supported that MSC-LIPUS had the highest bone volume/tissue volume. Histomorphometry showed a significantly faster remodeling in late phase in MSC-LIPUS and MSC groups. These indicated that the combined treatment of MSCs and LIPUS was beneficial to fracture healing. Regenerative power and homing ability of MSCs were shown by promotion in fracture healing and locally found green fluorescent protein (GFP)-labeled MSCs at fracture calluses. This evidence reflects that co-treatment of MSCs and LIPUS may be developed as an intervention for delayed union or nonunion. (E-mail: [louis@ort.cuhk.edu.hk](mailto:louis@ort.cuhk.edu.hk)) © 2013 World Federation for Ultrasound in Medicine & Biology.

**Key Words:** Mesenchymal stem cells, Low intensity pulsed ultrasound, Fracture healing, Migration.

### INTRODUCTION

Fracture healing is a regenerative process that follows a well-orchestrated sequence. Most fracture healing is uneventful because it is a mature biologic process. However, the healing process usually takes several weeks to complete and complications such as delayed unions and non-unions may occur in up to 10%–20% (Rodriguez-Merchan and Forriol 2004). Therefore, enhancement of fracture healing is one of the major objectives for orthopaedic surgeons as it is critical for the recovery and regain of functions after fracture. After the inflammation phase during the process of fracture healing, the callus is invaded by mesenchymal stem cells (MSCs) and blood vessels, while mechanical stimuli will sensitize these cells to differentiate to osteoblasts for bone formation (Einhorn 1998). Therefore, supply of MSCs and proper mechanical stimulation play a key role in the success of fracture healing.

Research on using exogenous MSCs as an intervention to enhance bone repair is scarce. MSCs have regenerative potential, making it an attractive approach to treat nonunion. A study reported that the application of exogenous MSCs could enhance fracture healing with biomechanical improvement through expressing bone morphogenetic protein-2 (BMP-2) and modulating the injury-related inflammatory response in mice model (Granero-Molto et al. 2009). Undale and co-workers also demonstrated that both human bone marrow MSCs and human embryonic stem cells (ESCs) could induce fracture healing in nonunion nude rats, whereas MSCs functioned more efficiently (Undale et al. 2011). The combined therapeutic effect of MSCs and low intensity pulsed ultrasound (LIPUS) on fracture repair is, however, lacking.

LIPUS has been proven to be effective in enhancing fracture healing by providing local acoustic mechanical stimulation. Several clinical trials demonstrated acceleration of healing in tibial fracture (Heckman et al. 1994), complex fracture (Leung et al. 2004b) and nonunion (Nolte et al. 2001; Jingshi et al. 2007). Together with positive *in vitro* data on human periosteal cells (Leung

Address correspondence to: Wing-Hoi Cheung, Ph.D., Department of Orthopaedics and Traumatology, 5/F, Clinical Sciences Building, The Chinese University of Hong Kong, Shatin, New Territories, Hong Kong SAR, China. E-mail: [louis@ort.cuhk.edu.hk](mailto:louis@ort.cuhk.edu.hk)

et al. 2004a) and human mesenchymal stem cells (Schumann et al. 2006), as well as *in vivo* evidences on bone regeneration (Claes and Willie 2007) and distraction osteogenesis (Chan et al. 2006), LIPUS is believed to modulate *in vivo* mechanical environment to exert a remarkable fracture healing enhancement.

In this study, we hypothesized that applications of exogenous MSCs and LIPUS could enhance fracture healing, compared with MSCs only. The objectives of this study were to investigate the combined effects of exogenous MSCs and LIPUS on fracture healing and to determine dynamic migration of MSCs to fracture site, with multiple analyses including radiography, micro-computed tomography (micro-CT), histomorphometry and *ex vivo* fluorescence imaging.

## MATERIALS AND METHODS

### *Animal model*

The Animal Experimentation Ethics Committee of the authors' institution approved the care and experimental protocol of this study (Ref. No. 07/010/ERG). In this study, 60 three-month-old female Sprague-Dawley (SD) rats obtained from the Laboratory Animal Services Center of the Chinese University of Hong Kong were used. All procedures were conducted by one experienced orthopedic surgeon. Unilateral closed femoral fractures were created at right femur shaft based on our established protocol (Leung et al. 2009; Cheung et al. 2011; Cheung et al. 2012), a modification from the Einhorn Protocol (Bonnarens and Einhorn 1984). Under general anaesthesia, a sterilized Kirschner wire (K-wire,  $\varnothing$  1.2 mm, Sanatmetal Ltd., Eger, Hungary) was inserted into the medullary canal retrogradely, following drilling and reaming with an 18 G needle ( $\varnothing$  1.27 mm). The K-wire then perforated the proximal femur through the piriformis fossa, and the tip was bent to leave a 3 mm length to prevent distal migration. The distal end of the K-wire was cut at the level of the articular surface to allow free joint movement. A custom-made 3-point-bending apparatus, with a metal blade (weighted 500 g) dropping from a height of 35 cm, was used to create the fracture at the midshaft of the femur. The quality of fracture with fracture gap smaller than 0.5 mm and displacement less than 0.5 mm was confirmed by anteroposterior (A-P) and lateral radiographies. For postoperative analgesia, single dose of buprenorphine (0.03 mg/kg, s.c.; Temgesic, Schering-Plough, NJ, USA) was given on a daily basis for the next 3 days. Rats were allowed unrestricted cage activities at all time.

### *Grouping and treatments*

The fractured rats were divided into three groups by blocked randomization: (1) MSC-LIPUS: intracardiac

injection of green fluorescent protein labeled MSCs (GFP-MSCs) plus LIPUS treatment group, (2) MSC: intracardiac injection of GFP-MSCs only group, and (3) CTL: no-treatment injection control group. The rats in MSC-LIPUS and MSC groups were anaesthetized by intraperitoneal injection of a mixture of ketamine (50 mg/kg) and xylazine (10 mg/kg) on day 3 post-fracture. GFP-MSCs were purchased from Cyagen Biosciences (Guangzhou, China), which were isolated from SD rats and transfected with GFP-expressing lentiviral construct. The cells were characterized with fluorochrome-conjugated antibodies specific to cell surface antigens CD29, CD34, CD44, CD45 and CD11b/c, which must show  $\geq 70\%$  positivity for expression of CD29 and CD44 and  $\leq 5\%$  positivity for expression of CD34, CD45 and CD11b/c, as well as their differentiative ability to osteocytes, adipocytes and chondrocytes. They were subcultured to the fifth passage, trypsinized and 4 million cells were suspended in 0.5 mL phosphate buffered saline (PBS). With confirmation of  $\geq 90\%$  viability of cells, a needle (23 G  $\times$  1<sup>1</sup>/<sub>4</sub>) was inserted percutaneously behind the forelimb and with the ultrasound positioning, the cells were infused into the left ventricle of the rats in 1 minute (Gibon et al. 2012). The rats in MSC-LIPUS group were then given daily LIPUS treatments (Exogen 3000+; Smith and Nephew Inc., Memphis, TN, USA) for 20 min/day, 5 days/week following the cell injection at day 3 post-fracture (Cheung et al. 2011, 2012). Ultrasound signal is of a 200  $\mu$ s burst of sine wave repeating at 1.0 kHz with 30.0 mW/cm. Under general anaesthesia (30 mg/kg ketamine and 5 mg/kg xylazine IP), the rats were laid on the ventral side and the LIPUS transducer was placed over the lateral side of the fracture site with a thin layer of coupling gel. For the MSC and CTL groups, the same treatment was performed except the LIPUS machines were turned off (sham treatment). Rats were euthanized by overdosed sodium pentobarbital at 1, 2, 3 and 4 weeks for end-point assessments including *ex vivo* fluorescence imaging, micro-CT, histomorphometry and immunohistochemistry ( $n = 5$  each for three groups and four time points), while weekly radiography was taken to monitor the healing status continuously. The assessors for these measurements were blinded to the grouping and time points during evaluation.

### *Radiologic analysis*

Fracture healing was monitored weekly on anteroposterior and lateral radiography (Faxitron X-ray system model 43855C; Faxitron. X-ray Systems, Wheeling, IL, USA), based on our established protocol (Leung et al. 2009; Cheung et al. 2011, 2012). Qualitatively, both the anteroposterior (AP) and lateral radiographs were assessed by two surgeons and the callus bridging was scored. Bone sample was counted as bridged if: (1)

bone bridging of the four cortices was observed in both AP and the lateral radiographs, and (2) consensus must be received from both surgeons. Quantitatively, the temporal changes of the callus morphology were measured using the lateral radiograph with Metamorph Image Analysis System (Universal Imaging Corporation, Downingtown, PA, USA). The callus width (CW) and the callus area (CA) were measured. CW was defined as the maximal outer diameter of the mineralized callus minus the outer diameter of the femur, whereas CA was the total sum of the external mineralized callus areas.

#### *Ex Vivo fluorescence imaging analysis*

After euthanasia at specific time points, the fracture samples were harvested. After soft tissue removal, the green fluorescent protein (GFP) measurements were performed and the fluorescent images were acquired. The fluorescence analysis was calibrated to the standard as recommended by the IVIS imaging operating manual (IVIS 200; Xenogen, Alameda, CA, USA). The intensities (in counts) were measured using the Live Image 2.5 software, with the settings of exposure time at 5 s, binning at 8 and f/stop at f/16 (Granero-Molto *et al.* 2009). A standard circular region-of-interest (ROI) with a diameter of 1 cm was defined around the callus area for all the measurements. After the background noise reduction, the intensities within the ROIs were used to calculate the average intensities.

#### *Micro-computed tomography (Micro-CT)*

Based on our established protocol (Leung *et al.* 2009; Cheung *et al.* 2012), micro-CT ( $\mu$ CT40; Scanco Medical, Brüttisellen, Switzerland) was used to scan the ROI at 5 mm proximal and distal to the fracture line. Three-dimensional (3-D) image of mineralized tissue was created using a low pass Gaussian filter (sigma = 1.2, support = 2). Tissue volume (TV) was defined and segmented from the two-dimensional (2-D) image semi-automatically. The low-density bone volume (newly formed mineralized callus) was considered at threshold 165–350; high-density bone volume (old cortices) was considered at 350–1000, while empty space was considered at 0–164, according to our established protocol modified from Gabet's one (Gabet *et al.* 2004). Bone volume fraction (bone volume/total bone volume or BV/TV) was calculated.

#### *Histomorphometric analysis*

The harvested samples were fixed in 10% neutral buffered formalin and then in 8% formic acid for decalcification. The femora were cut into halves along the mid-sagittal plane. The specimens were embedded in paraffin. Sectioned samples at 7  $\mu$ m in thickness were mounted on the silane coated glass slides and were

stained with hematoxylin-eosin (H&E). Qualitative assessment on endochondral ossification at the region 1.5 mm proximal and distal to the fracture line was performed. Quantitatively, the ratio (Cg.Ar/Cl.Ar) between the cartilage area (Cg.Ar) and the callus area (Cl.Ar) was measured (Leung *et al.* 2009; Cheung *et al.* 2012).

#### *Statistical analysis*

All quantitative data were expressed as mean  $\pm$  standard deviation and analyzed with SPSS v. 13.0 software (SPSS Inc., Chicago, IL, USA). Nonparametric Kruskal-Wallis test and post-hoc pairwise Mann Whitney tests were used to compare the differences among groups at the corresponding time points. Statistical significance was set at  $p \leq 0.05$ .

## RESULTS

#### *Radiologic analysis*

Radio-opaque external callus around fracture site was observed in both groups throughout the whole process. The weekly radiographies indicated that the fracture healed better in MSC-LIPUS and MSC groups than in CTL group. Callus bridging occurred on week 2 in both MSC-LIPUS and MSC groups, while CTL group started on week 3 (Fig. 1a). Quantitatively, both CW (Fig. 1b) and CA (Fig. 1c) in the MSC-LIPUS group were highest, the MSC group was in the middle and CTL group was the lowest. Kruskal-Wallis test indicated significant differences among groups for CW ( $p = 0.05, 0.006, 0.018, 0.020$  for weeks 1–4, respectively) and CA ( $p = 0.017, 0.007, 0.05$  and  $0.05$  for weeks 1–4, respectively) at all time points. MSC-LIPUS group showed significant increase in both CW and CA than CTL group at weeks 1–4 ( $p = 0.038$  for CW,  $p = 0.029$  for CA at week 1;  $p = 0.016$  for CW,  $p = 0.016$  for CA at week 2;  $p = 0.050$  for CW,  $p = 0.050$  for CA at week 3;  $p = 0.05$  for CW,  $p = 0.05$  for CA at week 4). Also, MSC-LIPUS group indicated significant increase in CW at week 4 ( $p = 0.05$ ) and CA at weeks 2–4 ( $p = 0.004, 0.010, 0.010$ , respectively) than MSC group. On the other side, MSC group demonstrated improved CW than CTL group at weeks 3–4 ( $p = 0.05$  for both).

#### *Ex vivo fluorescence imaging analysis*

GFP signal measurement indicated that the signals of each group kept a consistent level of readings with up to  $10^5$  counts along weeks 1–4, while the signals of MSC-LIPUS and MSC groups were obviously higher than CTL group. Quantitative analyses showed that there were significant differences among groups at all time points by Kruskal-Wallis test ( $p = 0.037, 0.035, 0.024, 0.037$  for weeks 1–4, respectively). Both MSC-LIPUS

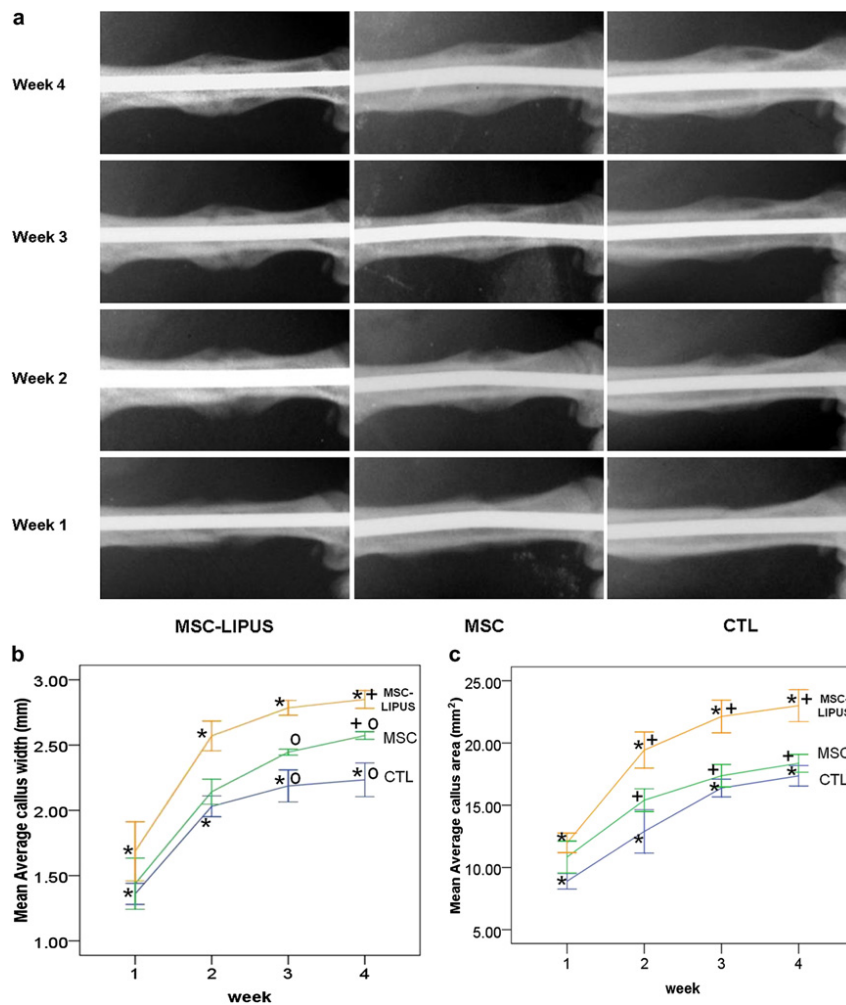


Fig. 1. Radiography and quantitative measurement of callus width (CW) and callus area (CA). (a) Serial radiography of the three groups at different time points. Mesenchymal stem cell-low intensity pulsed ultrasound (MSC-LIPUS) and MSC groups demonstrated callus bridging since week 2 but control (CTL) group started bridging at week 3. (b) CW of the three groups at different time points. MSC-LIPUS groups showed significantly higher CW than CTL group at all time points and MSC group at week 4. MSC group also indicated significantly higher CW than CTL group at weeks 3 and 4. (c) CA of the three groups at different time points. MSC-LIPUS groups showed significantly higher CA than CTL group at all time points and MSC group from weeks 2–4, whereas MSC group did not differ from CTL group at all time points. \* Denotes  $p \leq 0.05$  between MSC-LIPUS and CTL groups; + denotes  $p \leq 0.05$  between MSC-LIPUS and MSC groups; O denotes  $p \leq 0.05$  between MSC and CTL groups.

and MSC groups were significantly higher than CTL group at all time points with a range of 1.4–1.7-fold (MSC-LIPUS:  $p = 0.029$  for weeks 1–3 and 0.05 for week 4; MSC:  $p = 0.05$  for weeks 1–2 and 0.029 for weeks 3–4) (Fig. 2). There was, however, no difference between MSC-LIPUS and MSC groups.

#### Micro-computed tomography (micro-CT)

Reconstructed mineralized calluses showed different morphologic characteristics among groups at different time points. In general, 3-D micro-CT images showed the fastest closure of fracture gap in MSC-LIPUS group along weeks 1–4, while CTL group was the slowest (Fig. 3a). Quantitative analyses (Fig. 3b) re-

vealed that there were significant differences among groups at weeks 2–4 by Kruskal-Wallis test ( $p = 0.030, 0.039, 0.037$ , respectively). MSC-LIPUS group showed higher BV/TV values than CTL group at weeks 2–4 with significant differences (13.7%,  $p = 0.029$  for week 2; 10.2%,  $p = 0.029$  for week 3; 12.7%,  $p = 0.029$  for week 4). Meanwhile, MSC-LIPUS group also indicated a significantly higher BV/TV than MSC group by 9.0% at week 3 ( $p = 0.05$ ). However, there was no significant difference detected between MSC and CTL groups.

#### Histomorphometric analysis

All groups demonstrated secondary fracture healing with callus formation and endochondral ossification

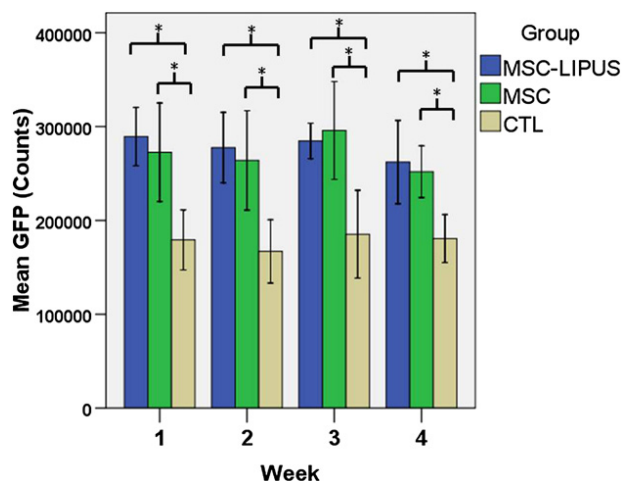


Fig. 2. *Ex vivo* GFP fluorescence counts at fracture callus of the three groups at different time points. Both mesenchymal stem cell-low intensity pulsed ultrasound (MSC-LIPUS) and MSC groups were significantly higher than control (CTL) group at weeks 1–4 (MSC-LIPUS:  $p = 0.029$  for week 1–3 and 0.050 for week 4; MSC:  $p = 0.050$  for weeks 1–2 and 0.029 for week 3–4). However, there was no difference between MSC-LIPUS and MSC groups. \*  $p < 0.05$ .

(Fig. 4a). Large amount of cartilaginous tissues bridged the osseous callus in the first week. At week 2, woven bone was observed in MSC-LIPUS and MSC groups with active endochondral ossification at the edge of cartilaginous tissues, while this phenomenon was shown in CTL group at week 3. The area of cartilaginous tissues tended to reduce in both MSC-LIPUS and MSC groups at week 3 and more woven bone replaced the cartilaginous tissues to bridge the fracture site in week 4, particularly in MSC-LIPUS group. There were, however, still large amounts of cartilaginous tissues in CTL group in week 4. Consistently, histomorphometric analysis demonstrated that there were significant differences among the groups at weeks 3–4 by Kruskal-Wallis test ( $p = 0.039, 0.015$ , respectively). The ratio of Cg.Ar/Cl.Ar was not different among the three groups at weeks 1 and 2, while both MSC-LIPUS and MSC groups indicated reduced Cg.Ar/Cl.Ar at weeks 3 and 4, compared with CTL group (Fig. 4b). At week 3, significant decrease was found in MSC-LIPUS group than in CTL group ( $-23.4\%$ ,  $p = 0.029$ ) and also observed in MSC group than CTL group ( $-7.8\%$ ,  $p = 0.029$ ). At week 4, significant difference was detected in both MSC-LIPUS ( $-67.6\%$ ,  $p = 0.029$ ) and MSC ( $-16.9\%$ ,  $p = 0.029$ ) groups over CTL group.

## DISCUSSION

The present study was designed to examine the combined effects of exogenous MSCs and LIPUS on fracture healing and to observe the dynamic migration

of exogenously injected MSCs to fracture site. The findings confirmed that co-applications of MSCs and LIPUS enhanced fracture healing better than MSCs only or CTL group, in terms of radiography, micro-CT and histomorphometry. This indicated that co-application of MSCs and LIPUS had a beneficial effect on fracture healing. *Ex vivo* GFP measurement also verified that the exogenous MSCs migrated to the fracture site, which reflected the homing ability of MSCs to injury sites. This is the first evidence showing the combined effects of exogenous MSCs and LIPUS for fracture repair, which is a potential interventional approach for delayed union or nonunion.

A more superior fracture healing effect was shown in MSC-LIPUS group with consistent findings in radiography, micro-CT and histomorphometry, compared with MSC only or CTL group. These reflected a beneficial effect of combined MSCs and LIPUS on callus formation (as indicated by CW and CA), new bone formation (as reflected by CW, CA, BV/TV and woven bone in histology) and accelerated bone remodeling (as shown by faster decrease of Cg.Ar/Cl.Ar in late phase) that facilitated fracture healing. To our best knowledge, there is no study reporting the combined effects of MSCs and LIPUS on fracture healing. Instead, the individual effect of exogenous MSCs or LIPUS only on fracture healing had been reported. Both interventions demonstrated beneficial effects on fracture healing. MSCs showed their regenerative capability for fracture repair by increasing callus biomechanical properties (Granero-Molto *et al.* 2009; Undale *et al.* 2011), while LIPUS was well confirmed to accelerate fracture healing by around 30% on average in many clinical trials (Khan and Laurencin 2008). The combined effect of MSCs and LIPUS may need further experiments to elucidate the detailed mechanism.

MSC only group also demonstrated better fracture healing than the CTL group in this study in most parameters with regard to CW (at weeks 3–4) and Cg.Ar/Cl.Ar (at weeks 3–4), despite the effects being not as good as MSC-LIPUS group. These confirmed the regenerative power of MSCs for fracture healing and substantiated with previously reported studies. The most related one by Granero-Molto *et al.* demonstrated that transplanted MSCs enhanced callus volume, new bone volume, hydroxyapatite content and biomechanical properties in mice (Granero-Molto *et al.* 2009), which was in accordance with our results. Undale's study also supported that exogenous MSCs could induce fracture healing by increasing biomechanical properties in nonunion nude rat model (Undale *et al.* 2011). Another one was applying MSCs onto ceramic carrier to treat critical-sized bone defects in adult athymic rats and the results revealed that new bone formation was detected from weeks 8–12

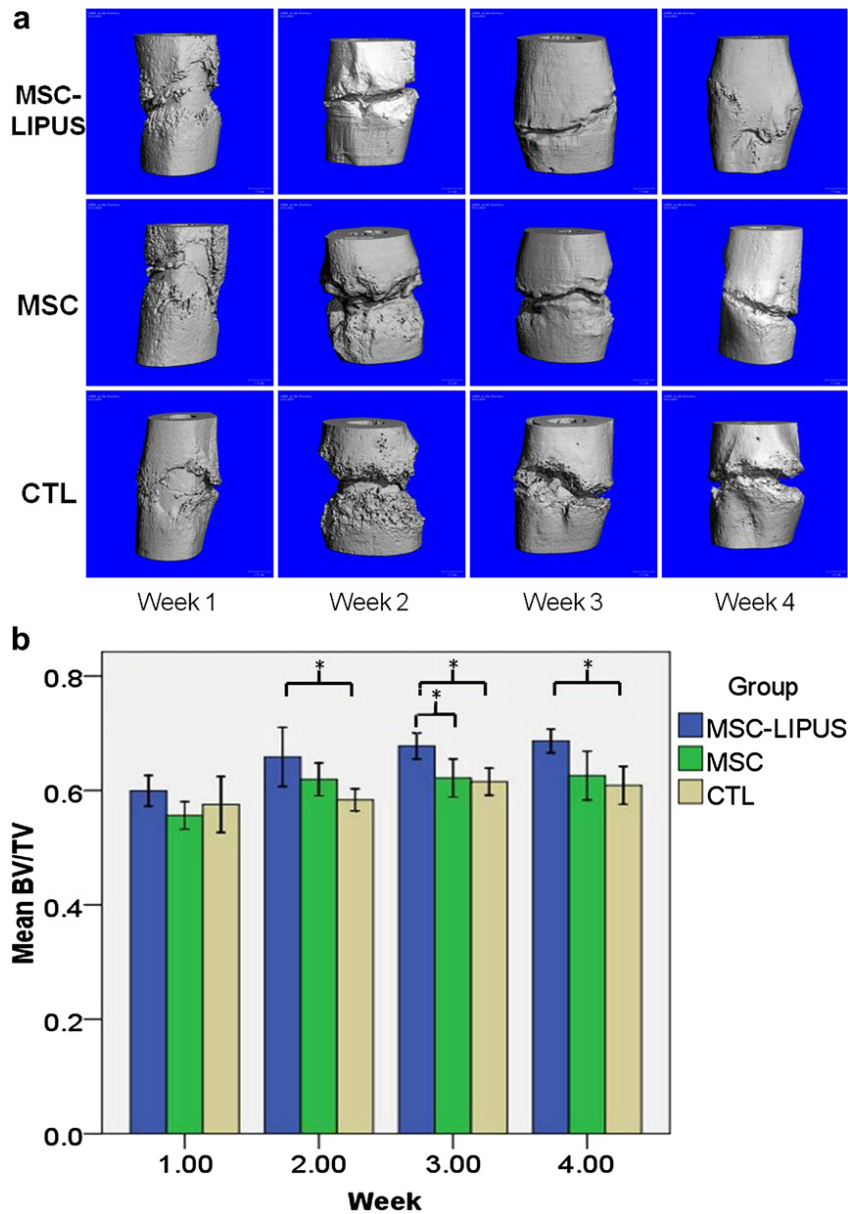


Fig. 3. Micro-CT images and quantitative measurement of bone volume/tissue volume (BV/TV). (a) Serial 3-D reconstructed micro-CT images of the three groups at different time points. Different morphologic changes of mineralized calluses were observed in the three different groups along the time points. Mesenchymal stem cell-low intensity pulsed ultrasound (MSC-LIPUS) group showed the fastest fracture healing with the fracture gap closure at week 4, whereas control (CTL) group indicated the slowest healing progress. (b) BV/TV of the three groups at different time points. MSC-LIPUS group demonstrated significantly higher BV/TV than CTL group at weeks 2–4 ( $p = 0.029$  for week 2–4) and MSC group at week 3 ( $p = 0.05$ ). No difference was found between MSC and CTL groups. \*  $p < 0.05$ .

as evaluated by radiography and histomorphometry with stronger biomechanical properties (Bruder et al. 1998).

LIPUS showed an enhancement effect on fracture healing, in addition to the regeneration by injected MSCs. Although this study did not look into the detailed mechanism, the past *in vitro* and *in vivo* evidences may provide some clues to explain the phenomenon. First, the potent ability of LIPUS to enhance cell proliferation and differentiation to osteogenic lineage of periosteal

cells, a critical cell type for fracture healing, is one potential mechanism (Leung et al. 2004a; Tam et al. 2008). Second, LIPUS could induce production of cytokines such as basic fibroblast growth factor (bFGF) and vascular endothelial growth factor (VEGF) (Doan et al. 1999; Reher et al. 1999) that are well known to enhance fracture healing. Also, LIPUS has been proven to increase blood flow around fracture site (Rawool et al. 2003) that might promote angiogenesis (Azuma et al. 2001; Cheung

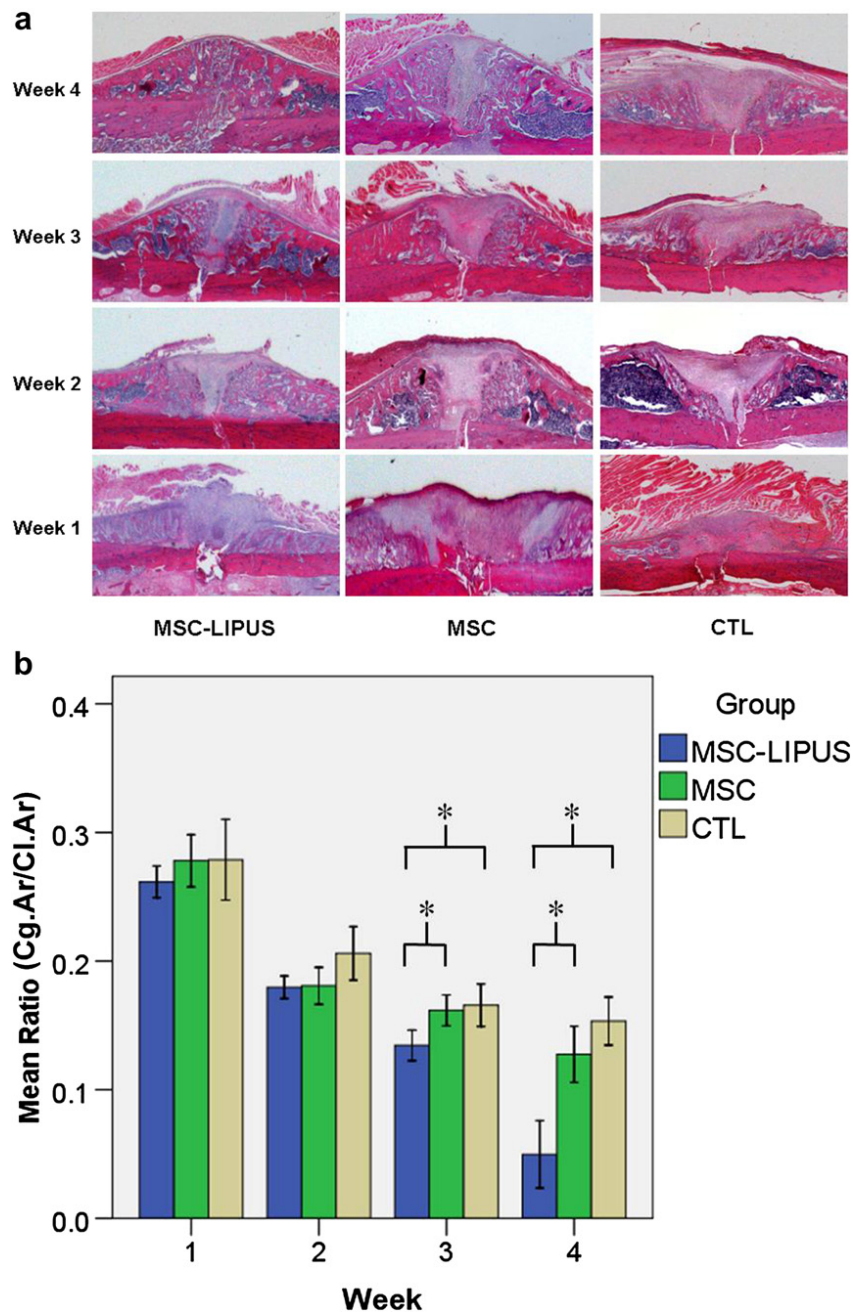


Fig. 4. Histology and histomorphologic analysis of cartilage area/callus area (Cg.Ar/Cl.Ar). (a) Serial histology of the three groups at different time points. At week 1, all groups showed large amount of chondroid tissues in the callus. At week 2, initiation of active endochondral ossification with woven bone formed was observed in Mesenchymal stem cell-low intensity pulsed ultrasound (MSC-LIPUS) and MSC groups. At week 3, the control (CTL) group started endochondral ossification, while reduction of chondroid tissues was observed in MSC-LIPUS and MSC groups. At week 4, almost no chondroid tissues were detected in MSC-LIPUS group; a large amount of chondroid tissues still existed in CTL group whereas MSC groups were between the two groups. (b) Cg.Ar/Cl.Ar of the three groups at different time points. There was no difference among the groups at week 1 and 2. At week 3, MSC-LIPUS and MSC groups showed significant decrease than CTL group ( $p = 0.029$  for both). At week 4, both MSC-LIPUS and MSC groups indicated significant decrease than CTL group ( $p = 0.029$  for both). \*  $p < 0.05$ .

*et al.* 2011), MSCs migration (Kumagai *et al.* 2012) and, hence, fracture healing.

The dynamic migration of MSCs to fracture site was assessed by *ex vivo* GFP imaging in this study, which both

MSC-LIPUS and MSC groups demonstrated similar levels of fluorescence counts at fracture site along all time points. This re-confirmed that MSCs have homing effect to the injury site, which was supported by many

previous studies (Devine et al. 2002; Shirley et al. 2005; He et al. 2007). In this study, injection of MSCs was applied intracardially instead of intravenously because most MSCs may be lost in the lung *via* intravenous injection as the size of MSCs are relatively large that cannot easily pass through the pulmonary capillaries (Lee et al. 2009). MSCs injection through the left ventricle of the heart is to avoid entrapment in the lungs and more MSCs can be delivered to the fracture site (Gibon et al. 2012). Four million of GFP-MSCs were administered in this study, which the cell number was relatively high compared with other previous similar interventional studies for fracture healing using around  $10^5$  (Undale et al. 2011) to  $10^6$  MSCs (Granero-Molto et al. 2009). This cell number was used because the authors would like to ensure the MSCs were sufficient or even in excess for treatment purpose. However, this study design might lead to the results of insignificant difference of GFP counts between MSC-LIPUS and MSC groups. LIPUS might have the potential to enhance the cell migration to fracture site as discussed above but when the injected MSCs were in excess, the enhanced migration might be masked.

This study has limitations. The study design did not include a group of LIPUS only for pairwise comparison with other groups because we aimed to investigate the effects of exogenous MSCs and LIPUS on fracture healing compared with MSCs only. Furthermore, since the effect of LIPUS on fracture healing has been widely reported before (Azuma et al. 2001; Cheung et al. 2011, 2012), we did not repeat it. Another limitation was the lack of mechanical testing, because we focused on evaluating the morphologic, densitometric and histologic changes of fracture healing, as well as the localization of MSCs in fracture callus. Biomechanical data was needed in next stage to confirm the efficacy of combined treatment on bone strength.

In conclusion, this study confirmed that application of MSCs and LIPUS enhanced fracture healing, compared with MSCs only or no-treatment control, as proven by radiography, micro-CT and histomorphometry. The combined effects of MSCs and LIPUS might be contributed by regenerative power of MSCs and LIPUS-induced cytokine production or osteogenic differentiation. MSCs only could locate at fracture callus and also promote fracture healing, indicating the homing effects to injury site and regenerative ability of MSCs. These evidences implicate that application of MSCs and LIPUS has an intriguing potential to be an intervention for delayed union or nonunion treatment.

**Acknowledgments**—This study was partially supported by the OTC Foundation Research Fund (Ref. No. 2009-WHLG) and partially by AO Research Grant (Ref No. S-11-10C). The authors thank Mr. Chow Kwoon-Ho Simon for his help with the English editing.

## REFERENCES

- Azuma Y, Ito M, Harada Y, Takagi H, Ohta T, Jingushi S. Low-intensity pulsed ultrasound accelerates rat femoral fracture healing by acting on the various cellular reactions in the fracture callus. *J Bone Miner Res* 2001;16:671–680.
- Bonnarens F, Einhorn TA. Production of a standard closed fracture in laboratory animal bone. *J Orthop Res* 1984;2:97–101.
- Bruder SP, Kurth AA, Shea M, Hayes WC, Jaiswal N, Kadiyala S. Bone regeneration by implantation of purified, culture-expanded human mesenchymal stem cells. *J Orthop Res* 1998;16:155–162.
- Chan CW, Qin L, Lee KM, Zhang M, Cheng JC, Leung KS. Low intensity pulsed ultrasound accelerated bone remodeling during consolidation stage of distraction osteogenesis. *J Orthop Res* 2006;24:263–270.
- Cheung WH, Chin WC, Qin L, Leung KS. Low intensity pulsed ultrasound enhances fracture healing in both ovariectomy-induced osteoporotic and age-matched normal bones. *J Orthop Res* 2012;30:129–136.
- Cheung WH, Chow SK, Sun MH, Qin L, Leung KS. Low-intensity pulsed ultrasound accelerated callus formation, angiogenesis and callus remodeling in osteoporotic fracture healing. *Ultrasound Med Biol* 2011;37:231–238.
- Claes L, Willie B. The enhancement of bone regeneration by ultrasound. *Prog Biophys Mol Biol* 2007;93:384–398.
- Devine MJ, Mierisch CM, Jang E, Anderson PC, Balian G. Transplanted bone marrow cells localize to fracture callus in a mouse model. *J Orthop Res* 2002;20:1232–1239.
- Doan N, Reher P, Meghji S, Harris M. *In vitro* effects of therapeutic ultrasound on cell proliferation, protein synthesis, and cytokine production by human fibroblasts, osteoblasts, and monocytes. *J Oral Maxillofac Surg* 1999;57:409–419. discussion 420.
- Einhorn TA. The cell and molecular biology of fracture healing. *Clin Orthop Relat Res* 1998;S7–S21.
- Gabet Y, Muller R, Regev E, Sela J, Shteyer A, Salisbury K, Chorev M, Bab I. Osteogenic growth peptide modulates fracture callus structural and mechanical properties. *Bone* 2004;35:65–73.
- Gibon E, Batke B, Jawad MU, Fritton K, Rao A, Yao Z, Biswal S, Gambhir SS, Goodman SB. MC3T3-E1 osteoprogenitor cells systemically migrate to a bone defect and enhance bone healing. *Tissue Eng Part A* 2012;18:968–973.
- Granero-Molto F, Weis JA, Miga MI, Landis B, Myers TJ, O'Rear L, Longobardi L, Jansen ED, Mortlock DP, Spagnoli A. Regenerative effects of transplanted mesenchymal stem cells in fracture healing. *Stem Cells* 2009;27:1887–1898.
- He Q, Wan C, Li G. Concise review: Multipotent mesenchymal stromal cells in blood. *Stem Cells* 2007;25:69–77.
- Heckman JD, Ryaby JP, McCabe J, Frey JJ, Kilcoyne RF. Acceleration of tibial fracture-healing by noninvasive, low-intensity pulsed ultrasound. *J Bone Joint Surg Am* 1994;76:26–34.
- Jingushi S, Mizuno K, Matsushita T, Itoman M. Low-intensity pulsed ultrasound treatment for postoperative delayed union or nonunion of long bone fractures. *J Orthop Sci* 2007;12:35–41.
- Khan Y, Laurencin CT. Fracture repair with ultrasound: Clinical and cell-based evaluation. *J Bone Joint Surg Am* 2008;90(Suppl 1):138–144.
- Kumagai K, Takeuchi R, Ishikawa H, Yamaguchi Y, Fujisawa T, Kuniya T, Takagawa S, Muschler GF, Saito T. Low-intensity pulsed ultrasound accelerates fracture healing by stimulation of recruitment of both local and circulating osteogenic progenitors. *J Orthop Res* 2012;30:1516–1521.
- Lee RH, Seo MJ, Pulin AA, Gregory CA, Ylostalo J, Prockop DJ. The CD34-like protein PODXL and alpha6-integrin (CD49f) identify early progenitor MSCs with increased clonogenicity and migration to infarcted heart in mice. *Blood* 2009;113:816–826.
- Leung KS, Cheung WH, Zhang C, Lee KM, Lo HK. Low intensity pulsed ultrasound stimulates osteogenic activity of human periosteal cells. *Clin Orthop Relat Res* 2004a;418:253–259.
- Leung KS, Lee WS, Tsui HF, Liu PP, Cheung WH. Complex tibial fracture outcomes following treatment with low-intensity pulsed ultrasound. *Ultrasound Med Biol* 2004b;30:389–395.

- Leung KS, Shi HF, Cheung WH, Qin L, Ng WK, Tam KF, Tang N. Low-magnitude high-frequency vibration accelerates callus formation, mineralization, and fracture healing in rats. *J Orthop Res* 2009;27:458–465.
- Nolte PA, van der Krans A, Patka P, Janssen IM, Ryaby JP, Albers GH. Low-intensity pulsed ultrasound in the treatment of nonunions. *J Trauma* 2001;51:693–702. discussion 703.
- Rawool NM, Goldberg BB, Forsberg F, Winder AA, Hume E. Power Doppler assessment of vascular changes during fracture treatment with low-intensity ultrasound. *J Ultrasound Med* 2003;22:145–153.
- Reher P, Doan N, Bradnock B, Meghji S, Harris M. Effect of ultrasound on the production of IL-8, basic FGF and VEGF. *Cytokine* 1999;11:416–423.
- Rodriguez-Merchan EC, Forriol F. Nonunion: General principles and experimental data. *Clin Orthop Relat Res* 2004;419:4–12.
- Schumann D, Kujat R, Zellner J, Angele MK, Nerlich M, Mayr E, Angele P. Treatment of human mesenchymal stem cells with pulsed low intensity ultrasound enhances the chondrogenic phenotype *in vitro*. *Biorheology* 2006;43:431–443.
- Shirley D, Marsh D, Jordan G, McQuaid S, Li G. Systemic recruitment of osteoblastic cells in fracture healing. *J Orthop Res* 2005;23:1013–1021.
- Tam KF, Cheung WH, Lee KM, Qin L, Leung KS. Osteogenic effects of low-intensity pulsed ultrasound, extracorporeal shockwaves and their combination—An *in vitro* comparative study on human periosteal cells. *Ultrasound Med Biol* 2008;34:1957–1965.
- Undale A, Fraser D, Hefferan T, Kopher RA, Herrick J, Evans GL, Li X, Kakar S, Hayes M, Atkinson E, Yaszemski MJ, Kaufman DS, Westendorf JJ, Khosla S. Induction of fracture repair by mesenchymal cells derived from human embryonic stem cells or bone marrow. *J Orthop Res* 2011;29:1804–1811.